Article:
Zhou, H, Finkemeier, I, Guan, W et al. (11 more authors) (2018) Oxidative stress-triggered interactions between the succinyl- and acetyl-proteomes of rice leaves. Plant, Cell and Environment, 41 (5). pp. 1139-1153. ISSN 0140-7791

https://doi.org/10.1111/pce.13100

Oxidative stress-triggered interactions between the succinyl- and acetyl-proteomes of rice leaves

Heng Zhou[1], Iris Finkemeier[2], Wenxue Guan[1], Maria-Armineh Tossounian[3,4,5], Bo Wei[3,4,5,6,7], David Young[3,4,5], Jingjing Huang[3,4,5,6,7], Joris Messens[3,4,5], Xibin Yang[8], Jun Zhu[8], Michael H. Wilson[9], Wenbiao Shen[1], Yanjie Xie[1,9,*], Christine H Foyer[9,*]

[1] Laboratory Center of Life Sciences, College of Life Science, Nanjing Agricultural University, Nanjing 210095, China.

[2] Institute of Plant Biology and Biotechnology, Westfaelische Wilhelms University Muenster, 48149 Muenster, Germany

[3] VIB-VUB Center for Structural Biology, B-1050 Brussels, Belgium.

[4] Brussels Center for Redox Biology, B-1050 Brussels, Belgium.

[5] Structural Biology Brussels, Vrije Universiteit Brussel, B-1050 Brussels, Belgium.

[6] VIB-UGent Center for Plant Systems Biology, Technologiepark 927, B-9052 Ghent, Belgium.

[7] Department of Plant Biotechnology and Bioinformatics, Ghent University, Technologiepark 927, B-9052 Ghent, Belgium.

[8] Jingjie PTM Biolab (Hangzhou) Co. Ltd, Hangzhou 310018, China.

[9] Centre for Plant Sciences, Faculty of Biological Sciences, University of Leeds, Leeds, LS2 9JT, UK

Running title: Redox mediated succinylome/acetylome interactions

Summary Statement

Protein post-transcriptional modifications (PTMs) such as lysine succinylation and acetylation regulating protein functions in response to metabolic and environmental cues. Here

we provide the first evidence that many proteins in rice leaves involved in photosynthesis, primary and redox metabolism, and also ribosomal functions are acetylated and succinylated simultaneously. Crucially, exposure to oxidative stress altered these PTMs on a specific subset of the identified sites. Succinylation altered the activities of catalase and a glutathione s-transferase. Hence, lysine succinylation and acetylation regulate the activities of proteins involved in plant responses to oxidative stress.

* For correspondence E-mail
yjxie@njau.edu.cn, Fax +86-25-8439-6542
c.foyer@leeds.ac.uk, Fax +44(0)113 323 3144

ABSTRACT

Protein lysine acylations, such as succinylation and acetylation are important posttranslational modification (PTM) mechanisms, with key roles in cellular regulation. Antibody-based affinity enrichment, high-resolution LC-MS/MS analysis and integrated bioinformatics analysis were used to characterize the lysine succinylome (K_{suc}) and acetylome (K_{ace}) of rice leaves. In total, 2593 succinylated and 1024 acetylated proteins were identified, of which 723 were simultaneously acetylated and succinylated. Proteins involved in photosynthetic carbon metabolism such as the large and small subunits of RuBisCO, ribosomal functions and other key processes were subject to both PTMs. Preliminary insights into oxidant-induced changes to the rice acetylome and succinylome were gained from treatments with hydrogen peroxide. Exposure to oxidative stress did not regulate global changes in the rice acetylome or succinylome but rather led to modifications on a specific subset of the identified sites. De-succinylation of recombinant catalase (CATA) and glutathione S-transferase (OsGSTU6) altered the activities of these enzymes showing that this PTM may have a regulatory function. These findings not only greatly extend the list of acetylated and/or succinylated proteins but they also demonstrate the close cooperation between these PTMs in leaf proteins with key metabolic functions.

Key-words: catalase, glutathione S transferase, post-translational modifications, photosynthesis

INTRODUCTION

Protein post-transcriptional modifications (PTM) are dynamic and reversible protein processing events that occur in prokaryotic and eukaryotic cells (Rao et al. 2014). Over 450 distinct PTMs have been identified to date. These PTMs include acetylation, succinylation, malonylation, butyrylation, and propionylation. All depend on the respective acyl-CoA availability. Of these modifications, protein acylation, which occurs on lysine residues, is considered to be amongst the most important regulatory mechanisms for broadening and fine-tuning of protein functions (Xing and Poirier 2012). Acetylation of the ε-amino group of lysine has emerged as an effective biological strategy for regulating cell physiology, and was first reported for histone proteins over 50 years ago (Allfrey et al. 1964). This reversible PTM, which occurs on a large number of proteins, is regulated by specific protein lysine acetyltransferases or deacetylases (Choudhary et al. 2009; Zhang et al. 2011; Xing and Poirier, 2012; König et al. 2014a; Hartl et al. 2017). Lysine acetylation can have a strong impact on the biochemical functions of proteins because the transfer of the acetyl group to lysine masks the positive charge, which is important for enzyme catalysis, protein-protein interactions and protein-DNA interactions (Glozak et al. 2005). Early investigations concerning the functions of this PTM focused largely on histones, transcription factors and other nuclear regulators. Hence, lysine acetylation has well characterized functions in the regulation of gene expression, via the modulation of chromatin structure, in response to metabolic and environmental triggers. The discovery of the acetylation of large numbers of non-histone proteins that are involved in diverse processes such as metabolism, transcription, translation and folding, has greatly extended our understanding of biological functions of this PTM (Cloudhary et al. 2009; Finkemeier et al. 2011; Wu et al. 2011; Chen et al. 2012; Zhang et al. 2012; Zhao et al. 2013; Pan et al. 2014).

Progress on defining the lysine acetylome of plants has been relatively slow compared to other organisms. However, recent advances in antibody-based affinity enrichment and high sensitive mass spectrometry (MS)-based proteomic analysis have made substantial contributions to the global analysis of lysine acetylation in plants (Hosp et al. 2017). A large number of acetylated non-histone proteins with diverse biological functions have been identified in several plant species. For example, 2152 acetylation sites were recently identified on 1022 proteins in Arabidopsis leaves (Hartl

et al., 2017), and 1392 acetylation sites were identified on 684 proteins with diverse functions in strawberry leaves (Fang et al, 2015). Of the two plant mitochondrial acetylomes that have also been reported, one identified 243 lysine acetylation sites on 120 Arabidopsis proteins (König et al. 2014b). Many tricarboxylic acid cycle enzymes were found to be lysine acetylated as well as proteins of the respiratory chain. Other acetylated proteins have functions in photorespiration, amino acid and protein metabolism, as well as in redox regulation. A study on pea (Pisum sativum) identified 664 lysine acetylation sites on 358 proteins in (Smith-Hammond et al. 2014). A total of 1142 proteins have been identified from three independent studies on rice (Nallamilli et al. 2014; He et al. 2016; Xiong et al. 2016). Although lysine acetylation has been reported in several plant species, its regulation and impact on metabolism has been investigated only in a few studies in plants to date (König et al, 2014a; Hart et al., 2017).

Lysine residues can also be modified by succinylation, which was first reported for the active site of homoserine trans-succinylase (Rosen et al. 2004). In this case, the substrate for succinylation is the succinyl group derived from succinyl-CoA (Zhang et al. 2011). The addition of a succinyl group causes a greater change in charge on the lysine target residue (from +1 to -1) than that of an acetyl group (from +1 to 0). This in turn will promote a more substantial transformation in the chemical properties of the target protein with the PTM. Lysine succinylation is therefore a likely candidate for other novel and sophisticated regulation of cellular functions, including the coordination of metabolism and cell signaling. Lysine succinylation has been comprehensively studied in mammals, and multiple substrate proteins have been identified (Du et al. 2011; Zhang et al. 2011; Colak et al. 2013; Park et al. 2013). Similar to acetylation, there are histone succinylation sites in regions where these proteins make close contact with DNA, suggesting functions in gene regulation through effects on chromatin structure (Xie et al. 2012). In plants, several succinylomes have been reported (He et al. 2016; Jin and Wu, 2016; Zhen et al. 2016; Shen et al. 2016; Zhang et al. 2017). A more global understanding of the roles of lysine succinylation is hindered by the dynamic properties of the PTM and the lack of incisive analytical technologies.

Redox PTMs, which largely involve the thiol moiety of cysteine residues, are important mechanisms that control cellular regulation and signalling in all organisms. They are controlled by small oxido-reductase proteins called thioredoxins and

glutaredoxins (Go et al. 2015; Hancock, 2009; Paulsen and Carroll, 2010). Cysteine residues are able to undergo a number of reversible oxidation states including sulfenic acid, intra or inter-subunit disulfide bonds, S-cysteinylation, S-glutathionylation, S-nitrosylation, or they can be irreversibly oxidised into sulfinic and sulfonic acids (Couturier et al, 2013; Go et al, 2015). In many cases, these thiol-based redox PTMs function as molecular switches regulating protein functions. However, the effects of oxidative stress on other PTMs such as succinylation and acetylation have not been characterised.

In this study, we explored the interplay between lysine acetylation and succinylation in rice leaves. Raw MS data are available via ProteomeXchange with identifier PXD007175. Both PTMs were found on rice proteins with a diverse range of functions, including glyoxylate and dicarboxylate metabolism, photosynthesis and protein synthesis and processing. In vitro experiments showed that succinylation can alter the activities of recombinant catalase and glutathione S-transferanse. The data presented here demonstrate that there are considerable interactions between the leaf acetylome and succinylome. The data presented here lay the foundations for further functional analysis of lysine acetylation and succinylation in plant responses to oxidative stress.

MATERIALS AND METHODS

Plant materials and growth conditions

Rice (Oryza sativa. cultivar Wuyunjing 7) was kindly provided by Jiangsu Academy of Agricultural Sciences, Jiangsu Province, China. Rice seeds were surface-sterilized with 5% NaClO for 20 min, washed extensively with distilled water and then germinated in distilled water at 28ºC for 2 days. Germinated seeds were cultivated on half-strength ammonium-free Murashige and Skoog (MS) medium (Xie et al. 2015). Seedlings were grown in a growth chamber with a 16/8 h day/night regime and 150 μmol m^{-2} s^{-1} irradiance, and 28/25 ºC day/night regime. For oxidative stress treatments, 14-days-old rice seedlings were transferred to 1/2 MS medium in the absence or presence of 1 mM H_2O_2 for 6 days. Rice seedlings were then harvested for protein extraction.

Western blot analysis

Proteins were isolated from three different rice tissues: germinating seeds and the stems and leaves (14-days-old seedlings) and flag leaves (3-months-old plants). Proteins from homogenates of different rice tissues were subjected to SDS-PAGE using a 12.5% acrylamide resolving gel. The primary antibody (1:1000 dilution; PTM Biolabs, Hangzhou, China) used was commercially available antibody against acetyl-lysine residues or sucinyl-lysine residues (Wagner and Payne, 2013; Nallamilli et al. 2014). Secondary anti-horseradish peroxidase antibody was used at 1:10000 dilution.

To detect the presence of succinylation on Sirt5-treated and non-treated OsGSTU6 recombinant protein, 2 μg of each sample was loaded on a 12% non-reducing SDS-PAGE gel, and proteins were transferred to polyvinylidene difluoride (PVDF) membrane. The membrane was blocked at room temperature for 1 h in blocking buffer (0.1% Tween 20 and 3% bovine serum albumin in PBS), and incubated with mouse anti-succinyllysine antibody (1:1000 dilutions, PTM Biolabs, Hangzhou,

China) overnight at 4°C. After washing three times with PBST buffer (0.1% Tween20 in PBS buffer), the membrane was incubated with horseradish peroxidase-conjugated sheep anti-mouse antibody (1: 50,000 Dilutions, GE healthcare) for 1 h at 37°C. The membrane was washed with PBST buffer solution, and bands were visualized with enhanced chemiluminescence (ECL) reagents (PerkinElmer) through Gel Doc™ XR+ Gel Documentation System (BIO-RAD). The density of each band was determined via Image Lab™ Software.

Protein extraction, trypsin digestion and TMT labeling

The leaves of 14-day-old rice seedlings that in been grown in the absence or presence of H_2O_2 were ground in liquid nitrogen. The frozen powder was transferred to centrifuge tubes, lysis buffer containing 8 M urea, 10 mM dithiothreitol (DTT) and 1% Protease Inhibitor Cocktail set VI (Merck) was added. The extracts were sonicated three times on ice and the soluble proteins isolated by centrifugation at 20,000 g at 4 °C for 10 min. Soluble proteins were precipitated by adding cold 15% trifluoroacetic acid (TCA) and the mixture was incubated -20 °C for 2 h. After centrifugation of the mixtures at 4 °C for 10 min, the supernatants were discarded. The protein precipitates were washed three times with cold acetone. Proteins were re-dissolved in buffer containing 8 M urea, 100 mM borane-triethylamine complex (TEAB pH 8.0). Protein concentrations were determined using a 2-D Quant kit (GE Healthcare) according to the manufacturer's instructions.

Prior to digestion, the proteins in the solution were first reduced by the addition of 10 mM DTT with incubation for 1 h (37 °C). Proteins were then alkylated with 20 mM iodoacetamide (Sigma) with incubation at room temperature for 45 min in darkness. For trypsin digestion, the protein sample was diluted by adding 100 mM TEAB to urea concentration less than 2M. Finally, trypsin was added at 1:50 trypsin-to-protein mass ratio for the first digestion overnight and 1:100 trypsin-to-protein mass ratio for a second 4 h-digestion.

After trypsin digestion, peptides were desalted by Strata X C18 SPE column (Phenomenex) and vacuum-dried. Peptides were reconstituted in 0.5 M TEAB and processed according to the manufacturer's protocol for 6-plex TMT kit. Briefly, one unit of TMT reagent (Thermo, defined as the amount of reagent required to label 1 mg of protein) were thawed and reconstituted in 24 μl acetonitrile (ThermoFisher chemical). The peptide mixtures were then incubated for 2 h at room temperature and pooled, desalted and dried by vacuum centrifugation.

High performance liquid chromatography (HPLC) fractionation and affinity enrichment

Samples were separated into fractions using high pH reverse-phase HPLC with an Agilent 300 Extend C18 column (5 μm particles, 4.6 mm ID, 250 mm length). Briefly, peptides were first separated on a gradient of 2% to 60% acetonitrile in 10 mM ammonium bicarbonate (pH 10). Over 80 min the extracts were separated into 80 fractions. The 80 peptide fractions were then combined into 18 fractions for the total proteome analysis and into 6 fractions for the acyl-lysine enrichments. Peptides were dried by vacuum centrifugation. The tryptic peptides were dissolved in NETN buffer (100 mM NaCl, 1 mM EDTA, 50 mM Tris-HCl, 0.5% NP-40, pH 8.0) and were incubated with pre-washed antibody beads (PTM Biolabs, Hangzhou, China) to bind K_{ace} or K_{suc} peptides, respectively. The mixtures were incubated at 4°C overnight with gentle shaking. The beads were then washed four times with NETN buffer and twice with double-distilled H_2O. The bound peptides were eluted from the beads with 0.1% trifluoroacetic acid (Sigma-Aldrich) and then and vacuum-dried. The resulting peptides were desalted with C18 ZipTips (Millipore) according to the manufacturer's instructions.

Proteomic analysis by liquid chromatography mass spectrometry (LC-MS/MS)

Peptides were dissolved in 0.1% formic acid (Fluka), directly loaded onto a reversed-phase pre-column (Acclaim PepMap 100, Thermo Scientific). Peptide

separation was performed using a reversed-phase analytical column (Acclaim PepMap RSLC, Thermo Scientific). The gradient comprised of 5% to 25% solvent B (0.1% formic acid in 98% acetonitrile) for 40 min, 25% to 35% for 10 min and climbing to 80% in 6 min then holding at 80% for the last 4 min, all at a constant flow rate of 270 nl/min on an EASY-nLC 1000 ultrahigh performance liquid chromatography (UPLC) system coupled to a Q Exactive^{TM} Plus hybrid quadrupole-Orbitrap mass spectrometer (ThermoFisher Scientific). A data-dependent procedure that alternated between one MS scan followed by 20 MS/MS scans was applied for the top 20 precursor ions above a threshold ion count of 3E6 in the MS survey scan with 15.0s dynamic exclusion and a 2.0 m/z isolation window. The electrospray voltage applied was 2.0 kV. MS spectra were aquired in the Orbitrap analyzer at a resolution of 70,000. HCD fragmentation was performed using NCE setting of 28, 32; ion fragments were detected in the Orbitrap at a resolution of 17,500. Automatic gain control (AGC) was used to prevent overfilling of the ion trap; 5E4 ions were accumulated for generation of MS/MS spectra. For MS scans, the m/z scan range was 350 to 1800. Fixed first mass was set as 100 m/z.

Database Searches

The resulting MS raw data were processed using MaxQuant (v.1.5.5.1) (Tyanova et al., 2016). Succinylation was added in the MaxQuant configurations with a mass of 100.01604 as modification on lysine residues allowed anywhere in the peptide. Acetylation of lysine residues was used as pre-defined, with C-term acetylation excluded. Tandem mass spectra were searched with the integrated Andromeda search engine against the Uniprot_OSjaponica 39947 database (63,195 sequences). Sequences of 248 common contaminant proteins and decoy sequences were automatically added during the search. Group specific parameters and fractions were defined for the whole proteome, succinyllysine- and acetyllysine-enriched samples, respectively. Oxidation on Met was set as variable modification in all parameter groups. Succinylation and acetylation on lysine were specified as variable

modifications within their respective parameter groups. A maximum number of five modifications per peptide were allowed. Trypsin specificity was required and a maximum of two (whole proteome) or four missed cleavages (acetylome, succinylome) were allowed. The minimal peptide length was set to seven amino acids. TMT6plex labels were defined as reporter MS2 ions at the N-terminus and lysine residues, respectively. TMT correction factors were defined in the configurations tab according to the manufacturer's instructions. In global parameters, carbamidomethylation on cysteine was specified as fixed modification. False discovery rate (FDR) thresholds for protein, peptide identifications were set to 1%. The minimum score for modified peptides was set to 40 and the minimum delta score for modified peptides was set to 6. All the other parameters in MaxQuant were set to default values, with a 20 ppm peptide tolerance in the first search and 4.5 ppm tolerance in the main search. The average mass standard deviation over all raw files was 0.92 ppm and the PIF (parent ion fraction: indicates the fraction the target peak makes up of the total intensity in the inclusion window) of all identified MS/MS spectra was 0.79 on average. Only peptides with a site localization probability of > 0.75 were retained. The mass spectrometry proteomics data were deposited on the ProteomeXchange Consortium via the PRIDE [1] partner repository with the dataset identifier PXD007175.

Bioinformatics annotation analysis

The Gene Ontology (GO), is a major bioinformatics initiative to unify the representation of gene and gene product attributes across all species. GO annotation proteome was derived from the UniProt-GOA database (www.http://www.ebi.ac.uk/GOA/). Firstly, identified protein IDs were converted to UniProt IDs and then mapped to GO IDs by protein ID. If some identified proteins were not annotated by UniProt-GOA database, the InterProScan soft was used to annotated protein's GO functional based on protein sequence alignment method (Dimmer et al. 2012). Then proteins were classified by Gene Ontology annotation based on three categories: biological process, cellular component and molecular function.

Identified proteins domain functional descriptions were annotated by InterPro domain database based on protein sequence alignment method. The InterPro domain database integrates diverse information about protein families, domains and functional sites, and makes it freely available to the public via web-based interfaces and services (Jones et al. 2014; Mitchell et al. 2015).

Kyoto Encyclopedia of Genes and Genomes (KEGG) connects known information on molecular interaction networks, such as pathways and complexes (the "Pathway" database), information about genes and proteins generated by genome projects (including the gene database) and information about biochemical compounds and reactions (including compound and reaction databases). KEGG database was used to annotate protein pathway (Moriya et al. 2007). Firstly, using KEGG online service tools, the KEGG automatic annotation server was used to annotate protein's KEGG database description. Then the annotation results were mapped on the KEGG pathway database using KEGG online service tools KEGG mapper.

WoLF PSORT, a subcellular localization predication soft, was used to predict subcellular localization, which is an updated version of PSORT/PSORT II for the prediction of eukaryotic sequences (Horton et al. 2007).

Functional enrichment analysis

Functional enrichment analyses of GO function, KEGG pathway and protein domain were performed to gain further insights into the involved function and pathways of the succinylated and acetylated proteins. For each category, Functional Annotation Tool of DAVID Bioinformatics Resources 6.7 was used to identify enriched clusters (Huang et al. 2009a; 2009b). A two-tailed Fisher's exact test was employed to test the enrichment of the protein-containing IPI entries against all IPI proteins. Correction for multiple hypothesis testing was carried out using standard false discovery rate control methods. Any terms with a corrected p-value < 0.05 was considered significant.

Motif Analysis

The Motif-X software was used to analyse the occurrence of amino acids in specific positions surrounding the modified lysine residues using 21-mers (10 amino acids upstream and downstream of the site) in all protein sequences. And all the database protein sequences were used as background database parameter, other parameters with default (Colak et al, 2013).

Protein-protein interaction network analysis.

Protein-protein interaction network was obtained from STRING database (Szklrczyk et al. 2011), and visualized using Cytoscape software (Shannon et al. 2003). A novel graph theoretical clustering algorithm, "Molecular Complex Detection" (MCODE), is part of the plug-in tool kit of the network analysis and visualization software Cytoscape. MOCODE core was used to detect densely connected regions in large protein-protein interaction networks, and cluster score > 10 was presented.

Recombinant Oryza sativa CATA and GSTU6 expression and purification

Catalase A (Q0E4K1) transcripts were amplified by PCR from O. sativa cDNA. After restriction digest, CATA was cloned into pPICZαA vector with EcoRI and BamHI restriction sites, and the recombinant CATA-c-myc-His protein was expressed using P. pastoris (GS115) strain with methanol as inducer. After 5 days induction, the supernatant of the medium was collected by centrifugation and the protein was enriched by using ammonium sulfate precipitation. The final supernatant of CATA protein was loaded onto a 1 mL Ni-NTA column to obtain the pure CATA protein after discarding the ammonium sulfate by using dialysis in Tris-HCl (50 mM, pH 7.5). The protein in wash buffer was analyzed by SDS-PAGE and Western blotting.

OsGSTU6 (LOC_Os10g38700) gene was cloned in pDEST^{TM}17 using Gateway^{TM} cloning system and transformed into E. coli C41 (DE3). Cells were grown in Luria Broth (Duchefa Biochemie) at 37˚C, induced with 0.5 mM isopropyl β-d-1-thiogalactopyranoside (IPTG) at OD_{600} 0.8, and incubated overnight at 25˚C.

Cells were harvested by centrifugation using Avanti® J-26xp centrifuge (BECKMAN COULTER®) and resuspended in lysis buffer (50 mM Tris-HCl pH 8, 500 mM NaCl, 1 mM TCEP, 50 µg/mL DNaseI, 20 mM $MgCl_2$, 0.1 mg/mL AEBSF and 1 µg/mL leupeptin). Cells were lysed with a Sonics Vibra Cell™ (10 min, 30s pulse on/off), and the lysate was in-batch incubated for 1 h at 4˚C with Ni^{2+}-Sepharose™ 6 Fast Flow beads (GE healthcare) equilibrated in binding buffer (50 mM Tris-HCl pH 8, 500 mM NaCl, 1 mM TCEP). The beads were packed and an AKTA™ Pure system (GE healthcare, Life Sciences) was used to elute bound OsGSTU6 using the elution buffer (50 mM Tris-HCl pH 8, 500 mM NaCl, 1 mM TCEP, 0.5 M imidazole). To assess the purity of the eluted fractions, the samples were loaded on a 15% non-reducing SDS-PAGE and bands were visualized with InstantBlue protein stain. The collected fractions were concentrated and further purified on Superdex75 16/90 column equilibrated in 20 mMTris-HCl pH 8 and 150 mM NaCl buffer solution. Non-reducing SDS-PAGE was used to assess the purity of the protein.

In vitro desuccinylation reactions for OsCATA and OsGSTU6

For each assay, 10-20 µg of the recombinant protein was treated with 4 µg of human SIRT5 and 60 µM NAD^+ in 25 mM Tris-HCl (pH 8) containing 137 mM NaCl, 2.7 mM KCl and 1 mM $MgCl_2$ in a 500 µL reaction volume. The samples were incubated for 1.5 h at 30˚C.

Enzymatic assays

CAT activity was determined according to the method of Aebi (1984). The reaction mixture contains 100 mM potassium phosphate buffer (pH 7.5) and CATA protein. The reaction was started by addition of 100 mM H_2O_2 and the enzyme activity was spectrophotometrically measured by monitoring the consumption of H_2O_2 (extinction coefficient 39.4 mM^{-1} cm^{-1}) at 240 nm.

To assess the glutathione S-transferase activity of GSTU6 in its succinylated and Sirt5-treated form, the conjugation of glutathione (GSH) on to 1-chloro-2,4-dinitrobenzene (CDNB) was monitored at 340 nm in function of time

using a SpectraMax340PC 96-well plate reader (Molecular Devices). The reaction mixture included 0.8 µM OsGSTU6, 5 mM GSH and 2.5 mM CDNB in 250 mM MOPS, pH. 6.5, 150 mM NaCl. The reaction started following the addition of CDNB. The change in absorbance in function of time was measured and the initial velocities were recorded. The assay was performed in triplicates and the bar graph was generated using GraphPad Prism7.

OsGSTU6 model construction

A homology model of OsGSTU6 was prepared with the SWISS-MODEL server (Arnold et al. 2006; Biasini et al. 2014) using the structure of wheat glutathione-S-transferase (PDB ID 1GWC) (55% sequence identity) as a template. Succinylation of lysines were modeled in JLigand (Lebedev et al. 2012), and GSH placed through structural superposition of the glutathionylated structure of Arabidopsis GSTU23 (PDB ID 5FR4). All modeled structures were energy-minimized with the CHARMM web interface (Miller et al. 2008) and stereochemistry validated with MolProbity (Chen et al. 2010).

RESULTS AND DISCUSSION

Detection of lysine succinylation and acetylation in rice

Samples of rice seeds harvested 4 days after germination were analyzed using lysine succinylation-specific and acetylation-specific pan-antibodies, together with the stems and leaves of 14 day old rice seedlings, and flag leaves of rice harvested at heading time, to give an overview on the abundance of lysine succinylation and acetylation in different rice tissues. Lysine succinylation and acetylation was observed on various types of proteins in all the rice tissues analyzed (Fig. 1A), and to a similar extent as previously reported for the other plant samples (Finkemeier et al. 2011; Li et al. 2014; Fang et al. 2015; Kosono et al. 2015).

Proteome-wide analysis of lysine-succinylated peptides and proteins in rice

Since the lysine succinylome of rice leaves has not been reported to date, we performed a succinyl-lysine antibody-dependent enrichment on trypsinated peptides, followed by LC-MS/MS analysis (Fig. 1B). Our analysis yielded a total of 5502 succinylated-lysine sites on 2593 rice proteins (Supplementary Table S1). The 2593 identified succinyl-proteins accounted for about 6.4% of the total identified rice leaf proteins. It has to be noted that more than half of these sites have a succinylated lysine residue at the C-terminus of the peptide identified with a high score and a high confidence localization score. These peptides cannot be generated by tryspin cleavage and therefore have to be either C-termini of proteins or protein fragments or cleavage products from other proteases. Since such a high number of C-terminally succinylated peptides were observed, we found that this finding has to be reported and therefore C-terminal succinylation was allowed in the MaxQuant search. In comparison only a few hundred C-terminal acetylated peptides can be observed, which are usually regarded as a result from chemical acetylation during peptide processing. Therefore, lysine acetylation at the C-terminus is excluded in the standard MaxQuant configurations. To the best of our knowledge, only four succinylome studies on plants

have been reported to date (rice, He et al. 2016; tomato, Jin and Wu, 2016; Brachypodium distachyon, Zhen et al. 2016; Taxus, Shen et al. 2016). The number of identified proteins reported here is nearly 10-times larger than in previous reports for rice seeds (He et al. 2016), paving the way for a better understanding for functional analysis of succinylation in rice and in other plant species. The increase in knowledge concerning the lysine succinylome presented here can be ascribed to improvements in antibody efficiency and mass spectrometry sensitivity (Table 1). The degree of succinylation of rice proteins is more or less the same as that reported in bacteria or mammalian cells (5502/2593=2.12) (Du et al. 2011; Zhang et al. 2011; Xie et al. 2012). However, the number of identified succinylation sites and matched proteins may vary markedly amongst prokaryotes, mammals and plants.

Ribulose-1, 5- bisphosphate carboxylase (RubBisCO) is the most abundant protein in leaves, accounting for approximate 50% of soluble leaf protein in C3 plants. The large subunit of RuBisCO (P0C512) was extensively succinylated. This protein has up to sixteen independent succinyl-lysine residues, including K32, K146, K164, K174, K177, K183, K201, K227, K236, K252, K305, K334, K356, K463, K466, K474 (Supplementary Fig. S1). The representative MS/MS spectra of the sixteen RuBisCO lysine succinyl-peptides identified in this study are shown in Supplementary Fig. S2. These observations suggest that succinylation is an important PTM in the regulation of photosynthetic CO_2 assimilation and/or photorespiration in rice plants.

Functional enrichment analysis of the rice lysine succinylome

Our data indicates that protein lysine succinylation is important in the regulation of cellular metabolism. Enrichment analysis ($p < 0.001$) using the KEGG, GO, and InterPro domain was performed to investigate the possible roles of proteins that were preferred targets for lysine succinylation in rice. In addition to RuBisCO, other lysine-succinylated protein substrates were mainly involved in primary metabolism. This includes carbon metabolism (136), biosynthesis of amino acids (110), glycolysis (66), oxidative phosphorylation (57), carbon fixation in photosynthetic organisms (46), glyoxylate and dicarboxylate metabolism (42) and others (Fig. 1C, Supplementary

Table S2). In addition, ribosome functions (118) and aminoacyl-tRNA biosynthesis (37) were also found to be significantly enriched in KEGG pathway, suggesting the potential role of protein succinylation in the regulation of translation and protein biosynthesis.

GO enrichment analysis based on the biological process category showed that a wide range of cellular and metabolic processes were observed to be significant enriched in succinylated proteins (Supplementary Table S3). These results indicate a wide ranging impact of lysine succinylation as a novel PTM type in rice, particularly with regard to the regulation of most fundamental cellular processes. The succinylation of primary metabolism-related enzymes may be a conserved regulation pattern in different organisms (Li et al. 2014; Kosono et al. 2015; Pan et al. 2015).

The enrichment analysis of InterPro Domain and KEGG pathways highlights photosynthesis and carbon metabolism as susceptible to regulation by succinylation (Fig. 2A). Enriched lysine-succinylated substrates with functional domains include thioredoxin-like fold, thioredoxin domain, and NAD(P)-binding domain. In addition, enrichment was observed in protein domains of glutathione S-transferase, heat shock protein, aminoacyl-tRNA synthetase classes I and II, ribosomal protein S5 domain 2-type fold. Overall, nearly 70 % of all the identified lysine succinylated proteins were predicted to localize in either the chloroplasts or cytoplasm (Fig. 1D). These findings are consistent with previous reports showing that K_{suc} is a frequently occurring PTM in bacteria and mammalian cells (Du et al. 2011; Zhang et al. 2011; Xie et al. 2012).

Analysis of succinylated-lysine sequence motifs

Previous studies on eukaryotic and prokaryotic cells have found preferences for amino acid residues at particular positions surrounding the succinylated lysine (Park et al. 2013). The sequence motifs of the identified lysine succinylated sites were therefore analyzed using the Motif-X program. Of 5502 of the succinylated sites identified in this study, 4762 were found to include the amino acid sequence from -10 to +10 positions surrounding the succinylated lysine. 26 conserved motifs were

significantly overrepresented around the lysine succinylation sites, such as $K_{-9/-8/-7}L_{-1}K^{suc}$, $K_{-10/-9/-8}E_{-1}K^{suc}$, $K_{-8}Y_{-1}/F_{-1}K^{suc}$, $L_{-7}F_{-1}K^{suc}$, $V_{-2}E_{-1}K^{suc}$, $R_{-10/-9/-8/-7}K^{suc}$, $K_{-10/-9/-8/-7}K^{suc}$, $F_{-1}/Y_{-1}/M_{-1}/L_{-1}/E_{-1}/Q_{-1}/V_{-1}/K^{suc}$, $K^{suc}Y_{+1}$ (Fig. 2B, C). A survey of these motifs indicated that at least two distinct models of residues are present. The first type is valine (V), isoleucine (I), leucine (L), methionine (M), glutamine (Q), phenylalanine (F) and tyrosine (Y), which are non-polar amino acids mainly located upstream of K_{suc} sites. Of these, only Y is located in downstream of K_{suc} sites. Most of these conserved residues were located at the ± 1 positions of the K_{suc} sites. In the embryo of germinating rice seeds, Xiong et al. (2016) defined five sequence motifs. The preferred amino acids of Q and E at -1 position, and T and V at + 2 position. Only Q and E were also identified in this study.

The frequencies of K and R were the lowest at positions from -6 to -1 and highest at positions -10 to -7. These results suggested that succinylation is preferred at lysine residues that are adjacent to an alkaline residue with a long side-chain (K or R) in positions -10 to -7, and lacking these amino acids in position -6 to -1. Similar results were as observed for the succinylome of E. coli (Colak et al. 2013), T. gondii (Li et al. 2014) and B. subtilis (Kosono et al. 2015), showing that plants and bacteria may share common conserved motifs surrounding succinylated lysine sites.

Proteome-wide analysis of lysine-acetylated peptides and proteins in rice

In the present study, protein acetylation was also successfully detected in rice leaves (Fig. 1A). High throughput analysis revealed a total of 1669 unique lysine acetylation sites on 1024 proteins (Supplementary Table S4), providing a promising starting point for the biological study of lysine acetylation in different rice tissues. However, these 1024 identified acetyl-proteins account for only about 2.54% of the total rice proteins.

Similar to the succinylome data, both the large and small subunits of RuBisCO were extensively acetylated (P0C512 and Q2QTJ7). Fourteen and 3 acetyl-lysine residues were found in P0C512 and Q2QTJ7 in this study respectively (Fig. S2; Supplementary Table S4). This finding indicates that the K_{ace} and K_{suc} may cooperate

or compete with each other in the regulation of the same protein, and this is likely to occur with respect to the same site. The RuBisCO large and small subunits had already been identified as heavily acetylated proteins in strawberry and Arabidopsis (Finkemeier et al. 2011; Fang et al. 2015). Nine out of 14 acetylated sites of P0C512 were identified in Arabidopsis, indicating the conservation of Rubisco acetylation in different species. Deacetylation of RuBisCO resulted in a 40% increase in the maximum catalytic activity of the enzyme, which may in turn alter the rate of photosynthesis (Finkemeier et al. 2011). These results suggest that the action of protein lysine acetylases and deacetylases may have considerable functional significance for the chloroplast. Further studies have to determine the effects of protein acetylation on photosynthesis.

Functional enrichment and motif analysis of the rice lysine acetylome

A GO functional classification of the 1024 identified acetylated proteins was conducted based on their biological processes and molecular function. These acetylated proteins covered almost all cellular functions. With respect to biological processes, 629 and 625 respectively were involved in cellular and metabolic process proteins, 417 were involved in single-organism process, and 158 responded to stimulus (Supplementary Table S5). Within the category of molecular function, the largest group (579 proteins) of GO annotated acetylated proteins was involved in binding activities, suggesting that acetylation is an important PTM in protein-protein interactions and in DNA transcription in rice leaves. The second largest group (490 proteins) has catalytic activity, indicating that the acetylation of enzymatic proteins may regulate or influence metabolic pathways. These features are similar to those previously reported in rice seeds and seedlings, confirming the presence of this PTM in proteins with these functions in different rice tissues (He et al. 2016; Xiong et al. 2016).

KEGG pathway enrichment was further conducted to elucidate the biological functions of acetylated proteins ($p < 0.001$). As shown, the lysine-acetylated proteins identified in the present study were mainly enriched in terms of functions in carbon

metabolism, ribosome, glyoxylate and dicarboxylate metabolism, glycol-metabolism pathways, and photosynthesis (Fig. 3A). Enrichment was also observed in proteins involved in oxidative phosphorylation and amino acid biosynthesis. Interestingly, these results were very similar to those determined for the lysine succinylome. A large proportion (723 out of 1024 proteins) was overlapped with succinylome, indicating the possible cooperation between these PTMs in the regulation of metabolic pathways.

Subsequent analysis using the InterPro domain database identified the functions of lysine-acetylated proteins further in terms of protein domains, such as the thioredoxin-like fold, thioredoxin and NAD-binding domains, as well as proteins invovled in transcription and translation, and histone and aminoacyl-tRNA synthetase (Fig. 3B). Proteins with these enriched domains are important in central energy metabolism. The subcellular location profiles showed that approximate 67 % (681 proteins) of all lysine acetylated proteins located in cytoplasm and chloroplasts (Supplementary Fig. S3). These proteins have roles in carbon fixation, photosynthesis and primary metabolism, as well as in ribosome functions. Of the mitochondria-localized proteins, functions in oxidative carbon metabolism and glycol-metabolism were significantly enriched. These results showed that lysine acetylation occurred extensively in proteins involved in photosynthesis, carbon metabolism and associated pathways. Previous studies on the mitochondrial acetylomes in Arabidopsis and pea showed similar features (König et al. 2014b; Smith-Hammond et al. 2014). Taken together, these results indicate the importance of succinylation and acetylation in the PTM-mediated regulation of carbon metabolism in chloroplasts and mitochondria.

A total of 11 conserved motifs, with amino acid sequences from -10 to +10 surrounding the acetylated lysine, were extracted from 1024 acetylated peptides. These enriched motifs were $K_{-7}K^{ace}K_{+1}$, $K^{ace}K_{+1+2/+3/+7}$, $K^{ace}R_{+1/+2}$, $K^{ace}S/H/T/N_{+1}$, $K^{ace}H_{+1}$, $K^{ace}T_{+1}$, $K^{ace}N_{+1}$ (Fig. 3C), with the most abundant of $K^{ace}R_{+1}$ and $K^{ace}K_{+1}$ (Fig. 3D). A survey of these motifs indicated that at least two distinct types of pattern are present: involving either a positively charged residue such as lysine (K), arginine

(R) and histone (H), or a non-polar residue, such as serine (S), threonine (T), and asparagine (N). Most of these conserved residues were located at the +1 position of the K^{ace} site. A $K^{ace}H_{+1}$ model has been reported previously (He et al. 2016; Xiong et al. 2016). Taken together, these findings suggest conservation of lysine acetylation in different rice tissues. Although the position was different, R, H, and K were also highly conserved in S. roseosporus motifs (Liao et al. 2014). Furthermore, we could also observed that positively charged amino acids, such as K and R were excluded from -1 position of acetylated lysine, showing a similar pattern to the succinylome (Fig. 2B). However, acetylation is preferred at lysine residues surrounded by K or R at positions -10 to -7.

Crosstalk between the leaf succinylome and acetylome

Increasing evidence supports the notion of extensive PTM crosstalk in the regulation of non-histone proteins in bacteria and mammals (Rao et al. 2014; Kosono et al. 2015). This comparison of the succinylome and acetylome profiles of rice leaves shows that of 1024 acetylated proteins analyzed, 723 also undergo succniylation (Fig. 4A; Supplementary Table S6). In addition, 301 K_{ace}-specific proteins (Supplementary Table S7) and 1870 K_{suc}-specific proteins were identified as well (Supplementary Table S8). These two types of PTMs can therefore occur at the same protein lysine residue in rice plants. For example, the large subunit of RuBisCO has overlapping sites for succinylation and acetylation (Supplementary Fig. S2). Of the sixteen succinylation sites identified, 11 were also found to be acetylated (Supplementary Figure S1). This interaction may be highly dynamic and involved in the regulation of photosynthesis. Moreover, several pathways associated with photosynthesis were enriched and almost 43% of the succinylated or 41% acetylated proteins were localized in the chloroplast (Supplementary Fig. S3). Fig. 4C showing the extensive modification of reaction center proteins, and proteins involved in photosynthetic electron transport and ATP synthesis by succinylation and/or acetylation. These results highlight the importance of the cooperation of these two PTMs in photosynthesis (Fang et al. 2015; He et al. 2016).

Experimental evidence supports crosstalk between the succinylome and acetylome in rice seeds (He et al. 2016). In this case, the ribosome complex and glycolysis/gluconeogenesis-related proteins were significantly enriched in both acetylated and succinylated proteins (He et al. 2016). In this study, a large proportion of rice leaf ribosomal subunits were found to be modified both by succinylation and acetylation (Fig. 4D), consistent with previous results in rice, bacteria and in Arabidopsis (Wu et al. 2011; Pan et al. 2015; He et al. 2016). These findings suggest a fundamental role for succinylation and/or acetylation in proteins involved in protein synthesis and processing.

KEGG pathway enrichment analysis highlights the role of succinylation and/or acetylation in proteins involved in a wide range of metabolic processes, including primary metabolism and oxidative phosphorylation (Supplementary Table S2 and S9). Interestingly, both succinylation and acetylation were extensively found in proteins associated with primary metabolic pathways. Almost all of the enzymes involved in the glycolysis/gluconeogenesis TCA cycle and pentose phosphate pathway were modified both by succinylation and acetylation (Fig. 4B). The intensive succinylation and acetylation of the glycolytic enzymes and acetyl-CoA metabolism-related enzymes indicates sophisticated interactions between the two PTMs in rice (He et al. 2016; Zhen et al. 2016). It is possible to speculate that the activities of these PTMs-related enzymes could be regulated by both succinylation and acetylation.

Insights into succinylome and acetylome profile changes in response to oxidative stress

A multi-parallel, large-scale proteomic approach combining TMT-based proteomics, antibody-based affinity enrichment, followed by high-resolution LC-MS/MS analysis, was employed for the relative quantification of protein abundance changes versus protein succinylation and acetylation changes. It is important to note that due to high experimental costs, this analysis was performed only on a single biological replicate in rice leaves treated with hydrogen peroxide (H_2O_2). Although no definitive conclusions can be drawn from studies without biological replication, we used the

dataset to a first glimpse of the responsiveness of these modifications to H_2O_2-induced oxidative stress. Not wishing to over-interpret the data or overestimate regulation at single proteins or sites, which might be false-positively regulated, we undertook a global GO-term analysis on all sites, which were regulated after correction for protein abundance changes. This analysis permits an evaluation of overall trends in the regulation of functional categories rather than single proteins (Supplementary Table S10, S11). Only the sites that met the following considerations were regarded as having undergone a change at the acetylation/succinylation level: (1) a PTM site localization probability of more than 0.75 (class I) and $\log_2$ reporter intensity not less than 8 and (2) a cut-off change of 1.3 or 0.77 for the value of H_2O_2 treatment verses the control after correction for protein abundance change was denoted as increased or decreased, respectively. Of all the identified Kace and Ksucc sites, about 12-32 % showed an altered abundance in response to H_2O_2, while the majority of these sites (77-87 %) were rather decreased than increased in abundance upon stress. This shows that only specific Kace and Ksucc sites are responsive to oxidative stress and that the majority of all modified sites is actually not regulated.

The GO enrichment-based analyses of these regulates sites revealed an overrepresentation of proteins involved in protein translation and folding, photosynthesis and glycolytic process. Furthermore, an enrichment in K_{suc}-specific proteins involved in ATP synthesis, coupled proton transport and cellular responses to oxidative stress was observed, suggesting that succinylation might be involved in the cellular adaptation oxidative stress. In contrast, an enrichment in K_{ace}-specific proteins was observed in purine ribosomal large subunit and nucleosome assembly, suggesting that acetylation might also be involved in responses to oxidative stress.

K_{suc} regulates enzyme functions

Lysine deacetylation altered the activities of Rubisco, phosphoglycerate kinase, GAPDH, malate dehydrogenase (MDH), and Rubisco activase in Arabidopsis (Finkemeier et al. 2011; Hartl et al. 2017). For example, acetylation of lysine residues in MDH enhanced the activity of this enzyme in E.coli and in Arabidopsis

(Finkemeier et al. 2011; Venkat et al. 2017). While succinylation is similar to acetylation, it induces more substantial changes to the chemical properties of the protein target. In this study, protein succinylation was shown to be a much more widespread PTM than acetylation in rice leaves. It is possible that K_{suc} of leaf proteins might be important in the cellular response to oxidative stress. This PTM may serve to counteract/prevent the oxidative modification of leaf proteins. We speculated that the modification of K_{suc} might contribute to cellular redox homeostasis through changes in the activities of antioxidant enzymes. Peroxisomes are not only an important site of ROS processing by catalase (CAT) but they are also a major site of ROS production through the glycolate oxidase reaction during photorespiration (Mhamdi et al. 2012). Twelve proteins involved in the pathways of glyoxylate and dicarboxylate metabolism showed occupancy by both K_{suc} and K_{ace} (Fig. 5A and B). Of these, the intensity of K_{suc} at position 150 in catalase A1 (CATA, Q0E4K1) was markedly decreased (0.372) in response to oxidative stress. To verify whether CATA is succinylated, we produced an OsCATA-c-myc-his recombinant protein by using GS115 strain of P. pastoris. After purification, we found that CATA was succinylated in the yeast system (Fig. 6A). In order to investigate the impact of succinylation on the CATA catalase activity, human SIRT5, a NAD-dependent desuccinylase enzyme that is known to regulate diverse metabolic pathways (Park et al. 2013), was used to catalyze the CATA desuccinlyation reactions. Western-blot analysis was then conducted to compare SIRT5-treated and non-treated OSCATA succinylation status. The SIRT5 treatment led to a complete loss of CATA lysine succinylation, indicating that the lysine succinylation produced in yeast, probably including K_{150}, was removed by the SIRT5 treatment. Treatment of SIRT5 caused an increase in CAT activity of over 50%. It is important to note that the abundance of the CATA protein was not changed markedly by oxidative stress (Supplementary Table S10). These observations indicate modulation of the succinylation level of catalase K150 by oxidative stress, most likely through a decrease in one or more specific succinyltransferases, which might regulate the activity of the enzyme.

We also checked proteins, whose intensity of K_{suc} was not altered markedly by oxidative stress. The redox-regulated glutathione S-transferase, OsGSTU6 (Q8S718) was chosen because of the relative intensities of K_{suc} at position 55 or 241 were 1.12 or 1.01 following oxidative stress compared to controls. To study the impact of succinylation on glutathione-S-transferase activity, OsGSTU6 was treated with SIRT5 to desuccinylate the enzyme protein. Western blot analysis showed a decrease in band intensity in the SIRT5-treated samples, indicating a decrease in protein succinylation state (Fig. 6B). The OsGSTU6-dependent conjugation of GSH to CDNB was decreased from 100% to 45.7% following treatment with SIRT5. This result indicates that succinylation of OsGSTU6 regulates the S-transferase activity of the enzyme by increasing the rate of the catalyzed GSH conjugation to CDNB. According to a homology model for OsGSTU6, K55 is in a predicted conformation, which is away from the GSH binding-site. Succinylation at K55 is therefore not expected to directly perturb the active site (Fig. 6). However, succinylation of K55 clearly modulates the transferase activity of OsGSTU6, increasing the catalytic turnover relative to the SIRT5-treated (desuccinylated) enzyme.

CONCLUSIONS

The regulation of protein structure and function is executed by specific PTMs that facilitate a high degree of plasticity and control by environmental and metabolic stimuli. The data presented here greatly extend our current knowledge of two important and yet relatively poorly characterized PTMs in plants: succinylation and acetylation. The present study identified 2593 succinylated proteins and 1024 acetylated proteins in rice. Of these 723 proteins were acetylated and succinylated simultaneously, highlighting substantial overlap between these PTMs. Proteins with important roles in primary metabolism particularly photosynthetic carbon metabolism and in key cellular processes such as ribosomal functions were subject to both PTMs. Conserved succinylated motifs also had similarities to the acetylation motifs identified in rice, which have been shown to differ from those identified previously in bacteria and mammals. Although somewhat preliminary, these findings suggest the presence of H_2O_2-triggered interactions between the lysine succinylome and acetylome in rice leaves. Moreover, in vitro experiments demonstrated that succinylation has a profound influence on the activities of CATA and GSTU6 recombinant proteins. These findings provide the first evidence that lysine succinylation and acetylation regulate the activities of key proteins involved in plant responses to oxidative stress.

ACKNOWLEDGMENTS

This work was financially supported from the National Natural Science Foundation of China (grant no. 31670255), the Fundamental Research Funds for the Central Universities (grant no. KYZ201529), Natural Science Foundation of Jiangsu Province (grant no. BK20161447), the Priority Academic Program Development of Jiangsu Higher Education Institutions (PAPD), Vlaams Instituut voor Biotechnologie (VIB), FWO PhD aspirant grant to MAT, Fonds voor Wetenschappelijk Onderzoek Vlaanderen (FWO project G0D7914N: “Sulfenomics: oxidatieve schakelaars in planten. Hoe zwavelhoudende planteneiwitten via 'agressieve' zuurstof praten”), the equipment grant HERC16 from the Hercules foundation, China scholarship council PhD fellowship to BW and visiting fellowship to YX, and the Strategic Research Programme (SRP34) of the VUB granted to JM. CHF and YX thank the Royal Society (UK) for an International Exchange China NSFC cost share grant.

REFERENCES

Allfrey VG, Faulkner R, Mirsky AE (1964) Acetylation and Methylation of histones and their possible role in the regulation of RNA synthesis. Proc Natl Acad Sci USA **51:** 786–794

Arnold K, Bordoli L, Kopp J, Schwede T (2006) The SWISS-MODEL workspace: a web-based environment for protein structure homology modelling. Bioinformatics **22:** 195–201

Biasini M, Bienert S, Waterhouse A, Arnold K, Studer G, Schmidt T, Kiefer F, Gallo Cassarino T, Bertoni M, Bordoli L, Schwede T (2014) SWISS-MODEL: modelling protein tertiary and quaternary structure using evolutionary information. Nucleic Acids Res **42**, W252–W258

Chen VB. Arendall WB, Headd JJ, Keedy DA, Immormino RM, Kapral GJ, Murray LW, Richardson JS, Richardson DC (2010) MolProbity: all-atom structure validation for macromolecular crystallography. Acta Crystallogr D Biol Crystallogr **66:** 12–21

Chen Y, Zhao W, Yang J, Cheng Z, Luo H, Lu Z, Tan M, Gu W, Zhao Y (2012) Quantitative acetylome analysis reveals the roles of SIRT1 in regulating diverse substrates and cellular pathways. Mol Cell Proteomics **11:** 1048–1062

Choudhary C, Kumar C, Gnad F, Nielsen ML, Rehman M, Walther TC, Olsen JV, Mann M (2009) Lysine acetylation targets protein complexes and co-regulates major cellular functions. Science **325:** 834–840

Colak G, Xie Z, Zhu A, Dai L, Lu Z, Zhang Y, Wan X, Chen Y, Cha Y, Lin H, Zhao Y, Tan M (2013) Identification of lysine succinylation substrates and the succinylation regulatory enzyme CobB in Escherichia coli. Mol Cell Proteomics **12:** 3509–3520

Couturier J, Chibani K, Jacquot JP, Rouhier N (2013). Cysteine-based redox regulation and signaling in plants. Front Plant Sci 4:105

Dimmer E, Huntley R, Alam-Faruque Y, Sawford T, O'Donovan C, Martin M., …, Apweiler R (2012) The UniProt-GO annotation database in 2011. Nucleic

Acids Res **40:** D565–D570

Du J, Zhou Y, Su X, Yu JJ, Khan S, Jiang H, …, Lin H (2011) Sirt5 is a NAD-dependent protein lysine demalonylase and desuccinylase. Science **334:** 806–809

Fang X, Chen W, Zhao Y, Ruan S, Zhang H, Yan C, …, Cheng Z (2015) Global analysis of lysine acetylation instrawberry leaves. Front Plant Sci 6: 739

Finkemeier I, Laxa M, Miguet L, Howden A, Sweetlove L (2011) Proteins of diverse function and subcellular location are lysine acetylated in Arabidopsis. Plant Physiol **155:** 1779–1790

Go YM, Chandler JD, Jones DP (2015) The cysteine proteome. Free Radic Biol Med **84:** 227–245

Glozak M, Sengupta N, Zhang X, Seto E (2005) Acetylation and deacetylation of non-histone proteins. Gene **363:** 15–23

Hancock JT (2009) The role of redox mechanisms in cell signalling. Mol Biotechnol **43:**162–166

Hartl M, Füßl M, Boersema P, Jost JO, Kramer K, Bakirbas A, Sindlinger J, Plöchinger M, Leister D, Uhrig G, Moorhead GBG, Cox J, Salvucci ME, Schwarzer D, Mann M, Finkemeier I (2017) Lysine acetylome profiling uncovers novel histone deacetylase substrate proteins in Arabidopsis. Mol Sys Biol, in press

He D, Wang Q, Li M, Damaris N, Yi X, Cheng Z, Yang P (2016) Global proteome analyses of lysine acetylation and succinylation reveal the widespread involvement of both modification in metabolism in the embryo of germinating rice seed. J Proteome Res **15:** 879–890

Horton P, Park J, Obayashi T, Fujita N, Harada H, Adams-Collier C, Nakai K (2007) WoLF PSORT: protein localization predictor. Nucleic Acids Res **35:** W585–W587

Hosp F, Lassowskat I, Santoro V, De Vleesschauwer D, Fliegner D, Redestig H, Mann M, Christian S, Hannah MA, Finkemeier I (2017) Lysine acetylation in mitochondria: From inventory to function. Mitochondrion **33:** 58–71

Huang D, Sherman B, Lempicki R (2009a) Bioinformatics enrichment tools: paths toward the comprehensive functional analysis of large gene lists. Nucleic Acids Res **37:** 1–13

Huang D, Sherman B, Lempicki R (2009b) Systematic and integrative analysis of large gene lists using DAVID bioinformatics resources. Nat Protoc **4:** 44–57

Jones P, Binns D, Chang H, Fraser M, Li W, McAnulla C, …, Hunter S (2014) InterProScan 5: genome-scale protein function classification. Bioinformatics **30:** 1236–1240

Lebedev, AA, Young P, Isupov MN, Moroz OV, Vagin AA, Murshudov GN (2012) JLigand: a graphical tool for the CCP4 template-restraint library. Acta Crystallogr D **68**: 431–440

Li X, Hu X, Wan Y, Xie G, Li X, Chen D, Cheng Z, Yi X, Liang S, Tan F (2014) Systematic identification of the lysine succinylation in the protozoan parasite Toxoplasma gondii. J Proteome Res **13:** 6087–6095

Kosono S, Tamura M, Suzuki S, Kawamura Y, Yoshida A, Nishiyama M, Yoshida M (2015) Changes in the acetylome and succinylome of Bacillus subtilis in response to carbon source. PLoS ONE **10:** e0131169

König AC, Hartl M, Pham PA, Laxa M, Boersema PJ, Orwat A, Kalitventseva I, Plochinger M, Braun HP, Leister D, Mann M, Wachter A, Fernie AR, Finkemeier I (2014a) The Arabidopsis class II sirtuin is a lysine deacetylase and interacts with mitochondrial energy metabolism. Plant Physiol **164:** 1401-1414

König A, Hard M, Bosersema P, Mann M, Finkemeier I (2014b) The mitochondrial lysine acetylome of Arabidopsis. Mitochondrion **19:** 252–260

Mhamdi A, Graham N, Alison B (2012) Plant Catalases: Peroxisomal redox guardians. Arch Biochem Biophys 525: 181–194

Moriya Y, Itoh M, Okuda S, Yoshizawa A, Kanehisa M (2007) KAAS: an

automatic genome annotation and pathway reconstruction serve. Nucleic Acids Res **35:** W182–W185

Miller BT, Singh RP, Klauda JB, Hodoscek M, Brooks BR, Woodcock HL (2008). CHARMMing: a new, flexible web portal for CHARMM. J Chem Inf Model **48:** 1920–1929

Mitchell A, Chang H, Daugherty L, Fraser M, Hunter S, Lopez R, …, Rober D (2015) The InterPro protein families database: the classification resource after 15 years. Nucleic Acids Res **43:** D213–D221

Nallamilli B, Edelmann M, Zhong X, Tan F, Mujahid H, Zhang J, Nanduri B, Peng Z (2014) Global analysis of lysine acetylation suggests the involvement of protein acetylation in diverse biological processes in rice (Oryza sativa). PLoS ONE **9:** e89283

Pan J, Ye Z, Cheng Z, Peng X, Wen L, Zhao F (2014) Systematic analysis of the lysine acetylome in Vibrio parahemolyticus. J Proteome Res **13:** 3294–3302

Pan J, Chen R, Li C, Li W, Ye Z (2015) Global analysis of protein lysine succinylation profiles and their overlap with lysine acetylation in the marine bacterium Vibrio parahemolyticus. J Proteome Res **14:** 4309–4318

Paulsen CE, Carroll KS (2013) Cysteine-mediated redox signaling: chemistry, biology, and tools for discovery. Chemical reviews **113:** 4633–4679

Park J, Chen Y, Tishkoff DX, Peng C, Tan M, Dai L, Xie Z, Zhang Y, Zwaans BM, Skinner ME, Lombard DB, Zhao Y (2013) SIRT-5mediated lysine desuccinylation impacts diverse metabolic pathways. Molec Cell **50:** 919–930

Rinalducci S, Marrocco C, Zolla L (2015). Thiol-based regulation of glyceraldehyde-3-phosphate dehydrogenase in blood bank-stored red blood cells: a strategy to counteract oxidative stress. Transfusion **55:**499–506

Rao E, Thelen J, Miernyk J (2014) Is Lys-N^{ε}-acetylation the next big thing in post-translational modifications? Trends Plant Sci **19:** 550–553

Rosen R, Becher D, Bűttner K, Biran D, Hecker M, Ron E (2004) Probing the active site of homoserine trans-succinylase. FEBS lett. **577:** 386–392

Smith-Hammond C, Hoyos E, Miernyk J (2014) The pea seedling mitochondrial

Nε-lysine acetylome. Mitochondrion **19:** 154–165

Shannon P, Markiel A, Ozier O, Baliga NS, Wang JT, Ramage D, Amin N, Schwikowski B, Ideker T (2003) Cytoscape: a software environment for integrated models of biomolecular interaction networks. Genome Res **13:** 2498–2504

Szklarczyk F, Franceschini A, Kuhn M, Simonovic M, Roth A, Minguez P, Doerks T, Stark M, Muller J, Bork P, Jensen LJ, von Mering C (2011) The STRING database in 2011: functional interaction networks of proteins globally integrated and scored. Nucleic Acids Res **39:** D561–D568

Tyanova S, Temu T, Cox J (2016) The MaxQuant computational platform for mass spectrometry-based shotgun proteomics. Nat Protoc **11**(12): 2301-2319.

Wagner G, Payne R (2013) Widespread and enzyme-independent Nε-acetylation and Nε-succinylation of proteins in the chemical conditions of the mitochondrial matrix. J Biol Chem **288:** 29036–29045

Weinert BT, Scholz C, Wagner SA, Iesmantavicius V, Su S, Daniel JA, Choudhary C (2013) Lysine succinylation is a frequently occurring modification in prokaryotes and eukaryotes and extensively overlaps with acetylation. Cell Rep **4:** 842–851

Wu X, Oh M, Schwarz E, Larue C, Sivaguru M, Imai B, Yau P, Ort D, Huber S (2011) Lysine acetylation is a widespread protein modification for diverse proteins in Arabidopsis. Plant Physiol **155:** 1769–1778

Xie L, Liu W, Li Q, Chen S, Xu M, Huang Q, Zeng J, Zhou M, Xie J (2015) First succinyl-proteome profiling of extensively drug-resistant Mycobacterium tuberculosis revealed involvement of succinylation in cellular physiology. J Proteome Res **14:** 107–119

Xie Y, Mai Y, Xu S, Zhou H, Duan X, Cui W, Zhang J, Xu G (2015) Heme-heme oxygenase 1 system is involved in ammonium tolerance by regulating antioxidant defence in Oryza sativa. Plant Cell Environ **38:** 129–143

Xie Z, Dai J, Dai L, Tan M, Cheng Z, Wu Y, Boeke JD, Zhao Y (2012) Lysine succinylation and lysine malonylation in histones. Mol Cell Proteomics **11:**

100–107

Xing S, Poirier Y (2012) The protein acetylome and the regulation of metabolism. Trends Plant Sci **17:** 423–430

Xiong Y, Peng X, Cheng Z, Liu W, Wang G (2016) A comprehensive catalog of the lysine-acetylation targets in rice (Oryza sativa) based on proteomic analyses. J Proteomics **138:** 20–29

Zaffagnini M, Michelet L, Marchand C, Sparla F, Decottignies P, Le Marechal P, Miginiac-Maslow M, Noctor G, Trost P, Lemaire SD (2007). The thioredoxin-independent isoform of chloroplastic glyceraldehyde-3-phosphate dehydrogenase is selectively regulated by glutathionylation. FEBS J **274:**212–226

Zhang Z, Tan M, Xie Z, Dai Y, Zhao Y (2011) Identification of lysine succinylation as a new post-translational modification. Nature Cell Biol **7:** 58–63

Zhang K, Zheng S, Yang JS, Chen Y, Cheng Z (2013) Comprehensive profiling of protein lysine acetylation in Escherichia coli. J Proteome Res **12:** 844–851

Zhang Y, Wang G, Song L, Mu P, Wang S, Liang W, Lin Q (2017) Global analysis of protein lysine succinylation profiles in common wheat. BMC Genomics **18:** 309

Zhao D, Zou S, Liu Y, Zhou X, Mo Y, Wang P, Xu Y, Dong B, Xiong Y, Lei Q, Guan K (2013) Lysine-5 acetylation negatively regulates lactate dehydrogenase A and is decreased in pancreatic cancer. Cancer Cell **23:** 464–476

LEGENDS TO FIGURES

Figure 1. Characterization of lysine succinylation and acetylation in rice. Analysis of rice acetylations and functional annotation of lysine succinylome in rice. (A) Detection of Lys-succinylated and acetylated proteins in rice samples using anti-suc/ace-Lys antibody. Samples were collected from germinating seeds (lane 1), stems (lane 2), leaves of 14-days-old seedlings (lane 3), and flag leaves of 3-months-old seedlings (lane 4). (B) The workflow of integrated strategy for global mapping of lysine succinylation and acetylation in rice seedling leaves. (C and D) KEGG pathway enrichment analysis ($P < 0.001$) and subcellular localization of lysine-succinylated proteins identified in this study.

Figure 2. Properties of the succinylated domains and peptides in rice leaves. (A) InterPro domain enrichment of the succinylated proteins in rice ($P < 0.001$). (B) Succinylation sequence motifs and conservation of succinylation sites. Numbers of each identified motifs were shown in (C).

Figure 3. Properties of the acetylated domains and peptides in rice leaves. (A) KEGG pathway enrichment analysis of lysine-acetylated proteins in rice. (C) InterPro domain enrichment of the acetylated proteins in rice leaves ($P < 0.001$). (B) Acetylation sequence motifs and conservation of acetylation sites. (D) Numbers of each identified motifs.

Figure 4. Specific and overlap between succinylation and acetylation of rice leaf proteins. (A) Venn diagram showing the number of peptides and proteins with lysine acetylation alone, succinylation alone, or with both modifications. (B) Key enzymes with succinyl- and acetyl-PTMs in glycolysis, the TCA cycle and pentose phosphate pathways. Photosynthesis and related pathways (C) and ribosomal proteins (D) modified by either acetylation and succinylation or both. See abbreviations section

and Table S15 for details.

Figure 5. Significant enriched KEGG pathways in rice leaves upon oxidative stress. (A) KEGG pathway enrichment analysis of differentially regulated succinylation and acetylation proteins after TMT-labeled protein normalization. (B) Venn diagram for the number of proteins enriched in pathway of glyoxylate and dicarboxylate metabolism showing lysine succinylation alone, acetylation alone, or with both modifications.

Figure 6. Lysine succinylation affects enzyme activities of rice OsCATA (A) and OsGSTU6 (B) recombinant proteins. Upper panel, Western blots and SDS-PAGE analyses of purified recombinant proteins. The number above the band indicates relative abundance of the corresponding anti-succinylation intensity with respect to the SDS-PAGE loading control. Bottom panel, enzyme activities were measured after incubation with (+) or without (-) human SIRT5 desuccinylase enzyme for 90 min at 30°C. Asterisks indicate significant differences compared with control treatment without the addition of SIRT5 desuccinylase enzyme ($P < 0.001$).

Table 1. Lysine succinylome and acetylome identified in rice and other plants.

	Number of identified proteins	Number of identified sites	Reference
Lysine succinylation			
Oryza sativa	2593	5502	This study
Oryza sativa	261	665	He et al. 2016
Brachypodium distachyon L.	262	605	Zhen et al. 2016
Solanum lycopersicum	202	347	Jin et al. 2016
Taxus	193	325	Shen et al. 2016
Lysine acetylation			
Oryza sativa	1024	1669	This study
Oryza sativa	716	1337	Xiong et al. 2016
Oryza sativa	389	699	He et al. 2016
Oryza sativa	44	60	Nallmilli et al. 2014
Strawberry	684	1392	Fang et al. 2015
Glycine max	245	400	Smith-Hammond et al. 2014
Vitis inifera	97	138	Melo-Braga et al. 2012
Arabidopsis	1022	2057	Hartl et al. 2017
Arabidopsis	204	348	König et al. 2014a
Arabidopsis	74	91	Finkemeier et al. 2011
Arabidopsis	57	64	Wu et al. 2011

Supplemental Information

Table S1. All the succinylated proteins and peptides identified in this study.

Table S2. KEGG enrichment analysis of succinylated proteins.

Table S3. GO enrichment analysis of succinylated proteins.

Table S4. All the acetylated proteins and peptides identified in this study.

Table S5. GO analysis of acetylated proteins.

Table S6. Common proteins which both succinylated and acetylated in this study.

Table S7. K_{ace}-specific proteins in this study.

Table S8. K_{suc}-specific proteins in this study.

Table S9. KEGG pathway analysis of the acetylome.

Table S10. The differentially expressed proteins in this study.

Table S11. GO enrichment analysis of differentially expressed proteins.

Table S12. The differentially expressed succinylated sites and proteins under H_2O_2 stress.

Table S13. The differentially expressed acetylated sites and proteins under H_2O_2 stress.

Table S14. The biological process based on GO enrichment analysis of the differentially expressed succinylated and acetylated proteins.

Table S15. Representative enzymes showing succinylation and acetylation in Fig. 4A.

Fig. S1. A representative protein showing showing the overlap of succinylation and acetylation sites. The eleven lysine sites at 146, 164, 175, 183, 201, 252, 305, 334, 356, 466, and 474 are both modified by succinylation (Suc) and acetylation (Ace) in RBCL (Entry ID: P0C512).

Fig. S2. MS spectra of RuBisCO large subunit succinylation.

Fig. S3. Subcellular localization of lysine-acetylated proteins identified in this study.

Fig. S4. OsGSTU6 modeled structure. The cartoon representation of (A) desuccinylated and (B) succinylated OsGSTU6 is shown. In both structures,

glutathione (GSH) indicated in light green, is bound within the G-site, and K55, which is located very close to this site is indicated in yellow. K55 succinylation is shown in orange color in (B). Both GSH and K55 are shown in stick form and the figure was generated using PyMol.

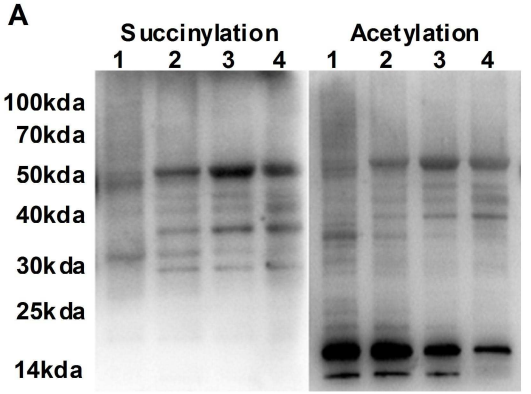
A
Succinylation
Acetylation
1 2 3 4
1 2 3 4
100kda
70kda
50kda
40kda
30kda
25kda
14kda

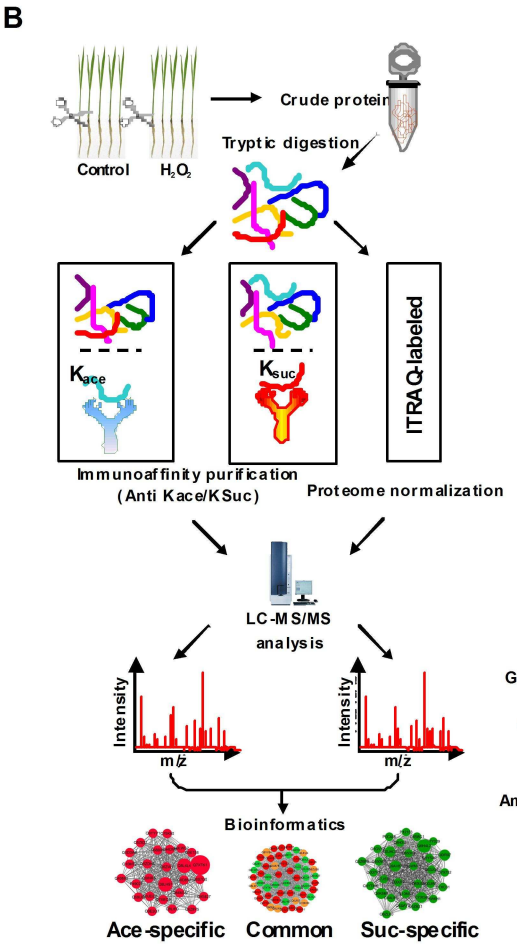
B
Crude protein
Tryptic digestion
Control
H_2O_2
K_{ace}
K_{suc}
ITRAQ-labeled
Immunoaffinity purification
(Anti Kace/KSuc)
Proteome normalization
LC-MS/MS
analysis
Intensity
m/z
Intensity
m/z
Bioinformatics
Ace-specific
Common
Suc-specific

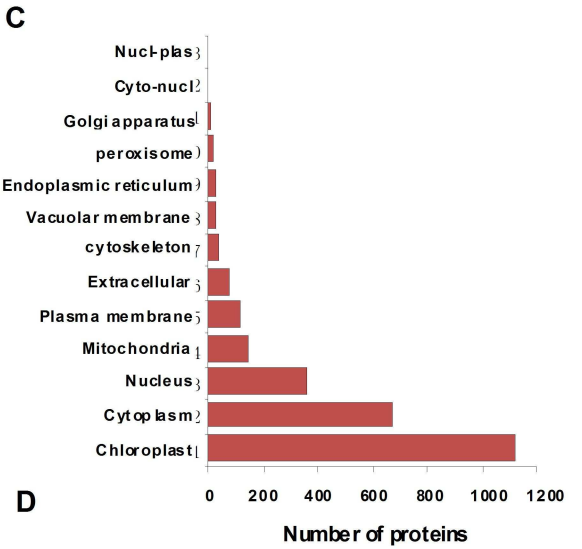
C
Nucl-plas 3
Cyto-nucl 2
Golgi apparatus 1
peroxisome 1
Endoplasmic reticulum 1
Vacuolar membrane 3
cytoskeleton 7
Extracellular 3
Plasma membrane 5
Mitochondria 11
Nucleus 33
Cytoplasm 22
Chloroplast 111
0 200 400 600 800 1000 1200
Number of proteins

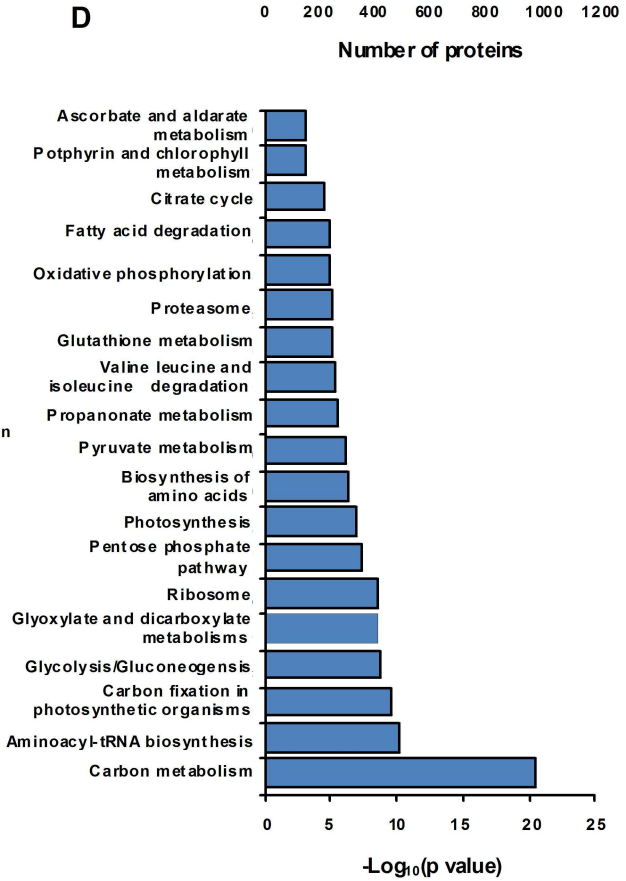
D
Ascorbate and aldarate metabolism
Potphyrin and chlorophyll metabolism
Citrate cycle
Fatty acid degradation
Oxidative phosphorylation
Proteasome
Glutathione metabolism
Valine leucine and isoleucine degradation
Propanonate metabolism
Pyruvate metabolism
Biosynthesis of amino acids
Photosynthesis
Pentose phosphate pathway
Ribosome
Glyoxylate and dicarboxylate metabolisms
Glycolysis/Gluconeogensis
Carbon fixation in photosynthetic organisms
Aminoacyl-tRNA biosynthesis
Carbon metabolism
0 5 10 15 20 25
-Log10(p value)

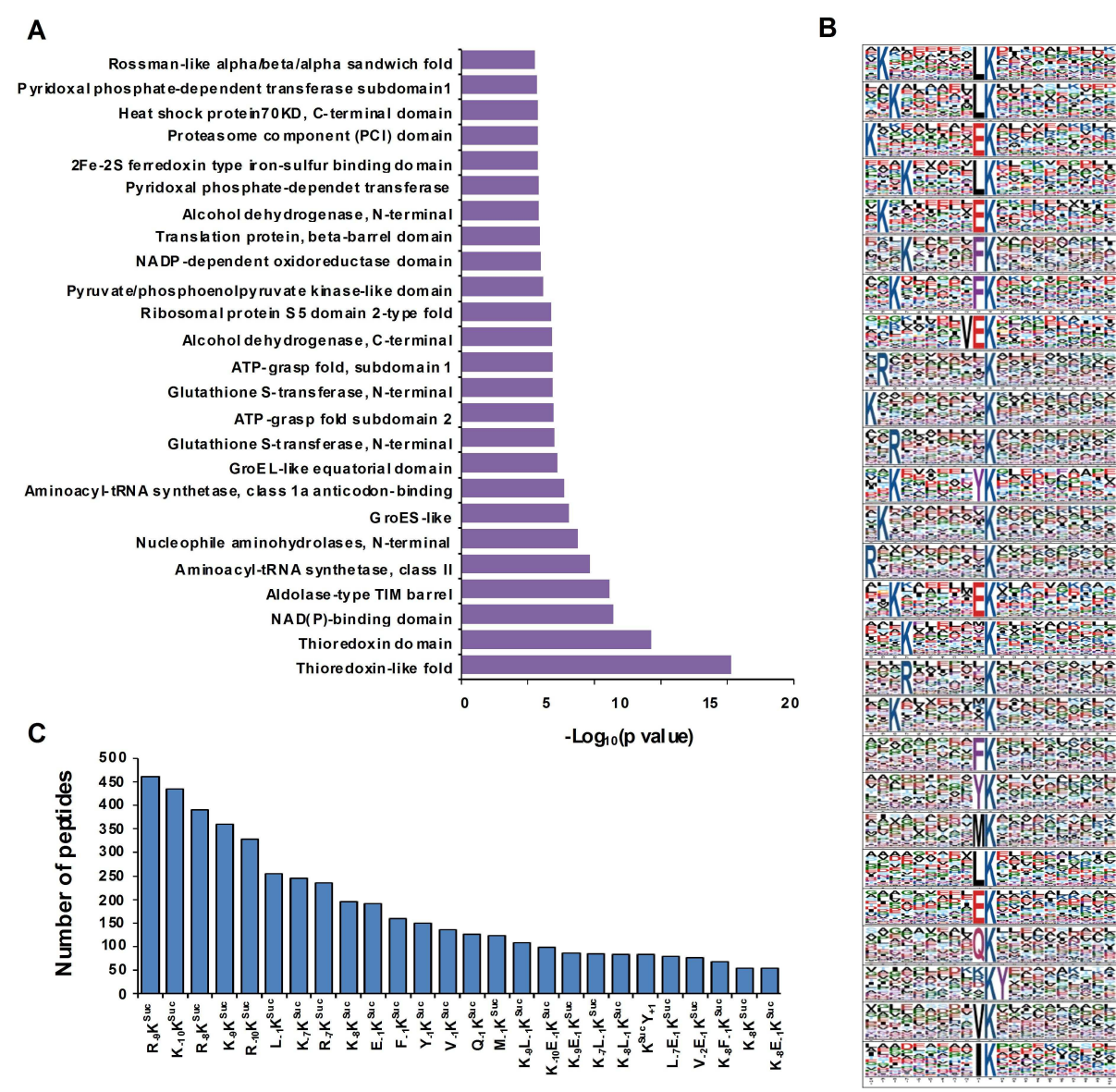
A
Rossman-like alpha/beta/alpha sandwich fold
Pyridoxal phosphate-dependent transferase subdomain1
Heat shock protein70KD, C-terminal domain
Proteasome component (PCI) domain
2Fe-2S ferredoxin type iron-sulfur binding domain
Pyridoxal phosphate-dependet transferase
Alcohol dehydrogenase, N-terminal
Translation protein, beta-barrel domain
NADP-dependent oxidoreductase domain
Pyruvate/phosphoenolpyruvate kinase-like domain
Ribosomal protein S5 domain 2-type fold
Alcohol dehydrogenase, C-terminal
ATP-grasp fold, subdomain 1
Glutathione S-transferase, N-terminal
ATP-grasp fold subdomain 2
Glutathione S-transferase, N-terminal
GroEL-like equatorial domain
Aminoacyl-tRNA synthetase, class 1a anticodon-binding
GroES-like
Nucleophile aminohydrolases, N-terminal
Aminoacyl-tRNA synthetase, class II
Aldolase-type TIM barrel
NAD(P)-binding domain
Thioredoxin domain
Thioredoxin-like fold
0
5
10
15
20
-Log10(p value)
B
C
Number of peptides
500
450
400
350
300
250
200
150
100
50
0
R-8KSuc
K-10KSuc
R-3KSuc
K-9KSuc
R-10KSuc
L-1KSuc
K-7KSuc
R-7KSuc
K-8KSuc
E-1KSuc
F-1KSuc
Y-1KSuc
V-1KSuc
Q-1KSuc
M-1KSuc
K-9L-1KSuc
K-10E-1KSuc
K-9E-1KSuc
K-7L-1KSuc
K-8L-1KSuc
KSucY+1
L-7E-1KSuc
V-2E-1KSuc
K-8F-1KSuc
K-8KSuc
K-8E-1KSuc

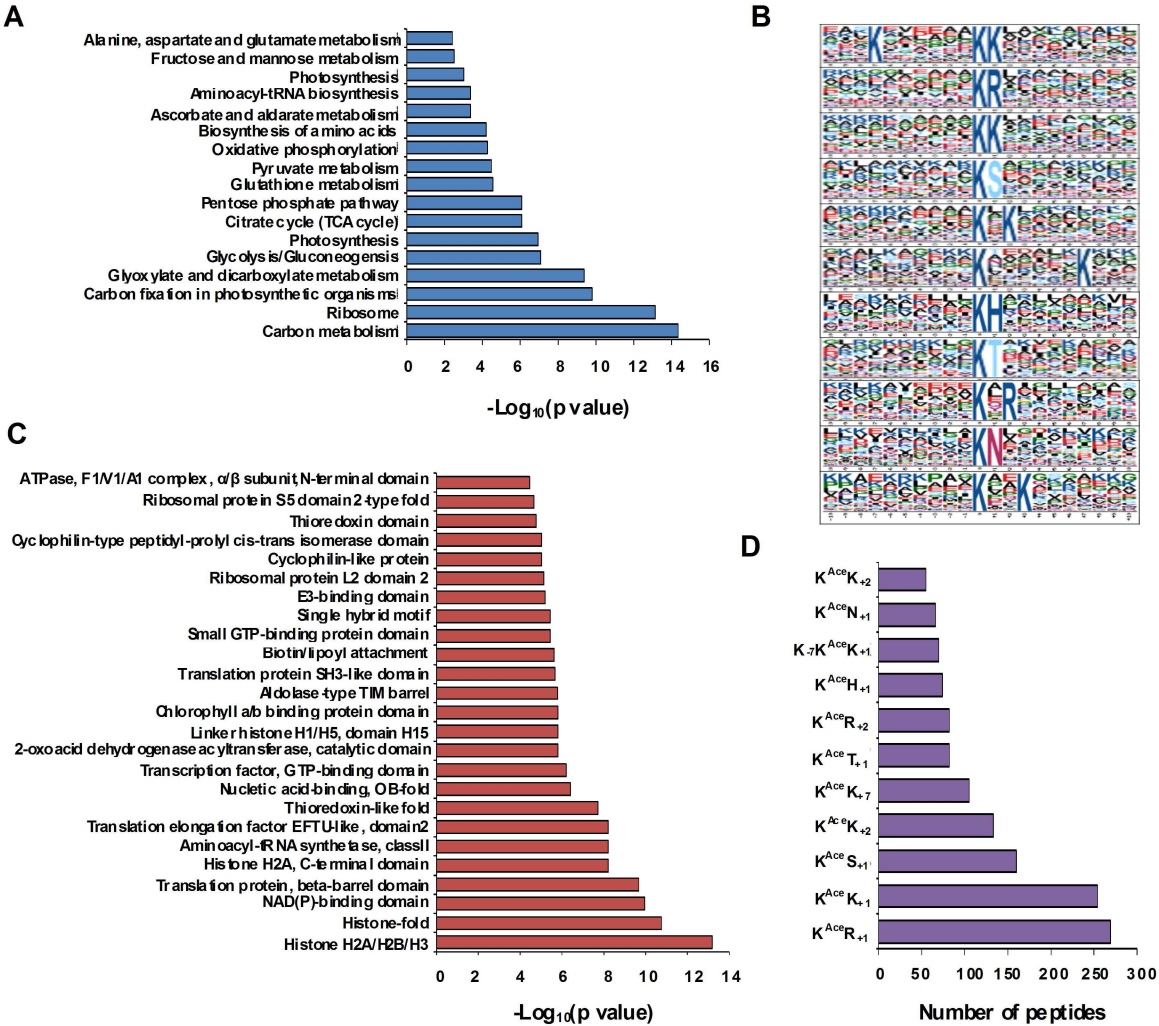
A
Alanine, aspartate and glutamate metabolism
Fructose and mannose metabolism
Photosynthesis
Aminoacyl-tRNA biosynthesis
Ascorbate and aldarate metabolism
Biosynthesis of amino acids
Oxidative phosphorylation
Pyruvate metabolism
Glutathione metabolism
Pentose phosphate pathway
Citrate cycle (TCA cycle)
Photosynthesis
Glycolysis/Gluconeogensis
Glyoxylate and dicarboxylate metabolism
Carbon fixation in photosynthetic organisms
Ribosome
Carbon metabolism
0 2 4 6 8 10 12 14 16
-Log10(p value)
B
C
ATPase, F1/V1/A1 complex, α/β subunit, N-terminal domain
Ribosomal protein S5 domain 2-type fold
Thioredoxin domain
Cyclophilin-type peptidyl-prolyl cis-trans isomerase domain
Cyclophilin-like protein
Ribosomal protein L2 domain 2
E3-binding domain
Single hybrid motif
Small GTP-binding protein domain
Biotin/lipoyl attachment
Translation protein SH3-like domain
Aldolase-type TIM barrel
Chlorophyll a/b binding protein domain
Linker histone H1/H5, domain H15
2-oxoacid dehydrogenase acyltransferase, catalytic domain
Transcription factor, GTP-binding domain
Nucleic acid-binding, OB-fold
Thioredoxin-like fold
Translation elongation factor EFTU-like, domain 2
Aminoacyl-tRNA synthetase, class II
Histone H2A, C-terminal domain
Translation protein, beta-barrel domain
NAD(P)-binding domain
Histone-fold
Histone H2A/H2B/H3
0 2 4 6 8 10 12 14
-Log10(p value)
D
K Ace K +2
K Ace N +1
K -7 K Ace K +1
K Ace H +1
K Ace R +2
K Ace T +1
K Ace K +7
K Ace K +2
K Ace S +1
K Ace K +1
K Ace R +1
0 50 100 150 200 250 300
Number of peptides

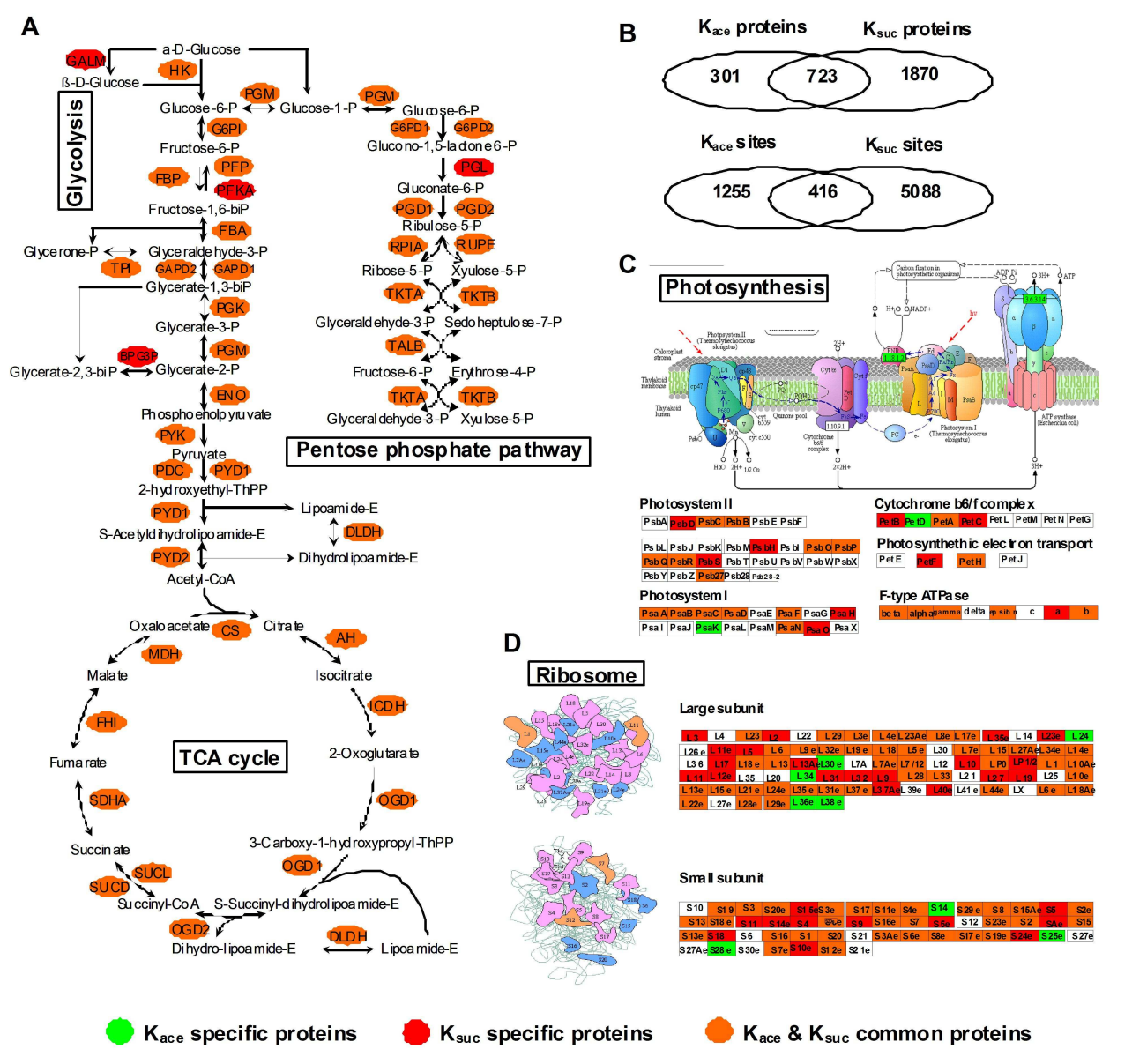
A
Glycolysis
a-D-Glucose
GALM
HK
ß-D-Glucose
Glucose-6-P
PGM
Glucose-1-P
G6PI
Fructose-6-P
FBP
PFP
PFKA
Fructose-1,6-biP
FBA
Glycerone-P
Glyceraldehyde-3-P
TPI
GAPD2
GAPD1
Glycerate-1,3-biP
PGK
Glycerate-3-P
BPG3P
PGM
Glycerate-2,3-biP
Glycerate-2-P
ENO
Phosphoenolpyruvate
PYK
Pyruvate
PDC
PYD1
2-hydroxyethyl-ThPP
PYD1
Lipoamide-E
S-Acetyldihydrolipoamide-E
DLDH
PYD2
Dihydrolipoamide-E
Acetyl-CoA
Oxaloacetate
CS
Citrate
MDH
AH
Malate
Isocitrate
FHI
IDH
Fumarate
TCA cycle
2-Oxoglutarate
SDHA
OGD1
Succinate
3-Carboxy-1-hydroxypropyl-ThPP
OGD1
SUCL
SUCD
Succinyl-CoA
S-Succinyl-dihydrolipoamide-E
OGD2
DLDH
Dihydro-lipoamide-E
Lipoamide-E
Glucose-6-P
G6PD1
G6PD2
Gluconolactone-6-P
PGL
Gluconate-6-P
PGD1
PGD2
Ribulose-5-P
RPIA
RUPE
Ribose-5-P
Xyulose-5-P
TKTA
TKTB
Glyceraldehyde-3-P
Sedoheptulose-7-P
TALB
Fructose-6-P
Erythrose-4-P
TKTA
TKTB
Glyceraldehyde-3-P
Xyulose-5-P
Pentose phosphate pathway
B
Kace proteins
Ksuc proteins
301
723
1870
Kace sites
Ksuc sites
1255
416
5088
C
Photosynthesis
Photosystem II
PsbA PsbD PsbC PsbB PsbE PsbF
PsbL PsbJ PsbK PsbM PsbH PsbI PsbO PsbP
PsbQ PsbR PsbS PsbT PsbU PsbV PsbW PsbX
PsbY PsbZ Psb27 Psb28 Psb28-2
Photosystem I
PsaA PsaB PsaC PsaD PsaE PsaF PsaG PsaH
PsaI PsaJ PsaK PsaL PsaM PsaN PsaO PsaX
Cytochrome b6/f complex
PetB PetD PetA PetC PetL PetM PetN PetG
Photosynthetic electron transport
PetE PetF PetH PetJ
F-type ATPase
beta alpha gamma delta epsilon c a b
D
Ribosome
Large subunit
L3 L4 L23 L2 L22 L29 L3e L4e L23Ae L8e L17e L35e L14 L23e L24
L26e L11e L5 L6 L9e L32e L19e L18 L5e L30 L7e L15 L27Ae L34e L14e
L3 6 L17 L18e L13 L13Ae L30e L7A L7Ae L7/12 L12 L10 LP0 LP1/2 L1 L10Ae
L11 L12e L35 L20 L34 L31 L21 L9 L28 L33 L21 L37 L19 L7 L10e
L13e L15e L21e L24e L35e L31e L37e L37Ae L39e L40e L41e L44e LX L6e L18Ae
L22e L27e L28e L29e L36e L38e
Small subunit
S10 S19 S3 S20e S15e S3e S17 S11e S4e S14 S29e S8 S15Ae S5 S2e
S13 S18e S11 S14e S4 S9e S9 S16e S7 S5e S12 S23e S2 SAe S15
S13e S18 S6 S16 S1 S20 S21 S3Ae S6e S8e S17e S19e S24e S25e S27e
S27Ae S28e S30e S7e S10e S12e S21e
Kace specific proteins
Ksuc specific proteins
Kace & Ksuc common proteins

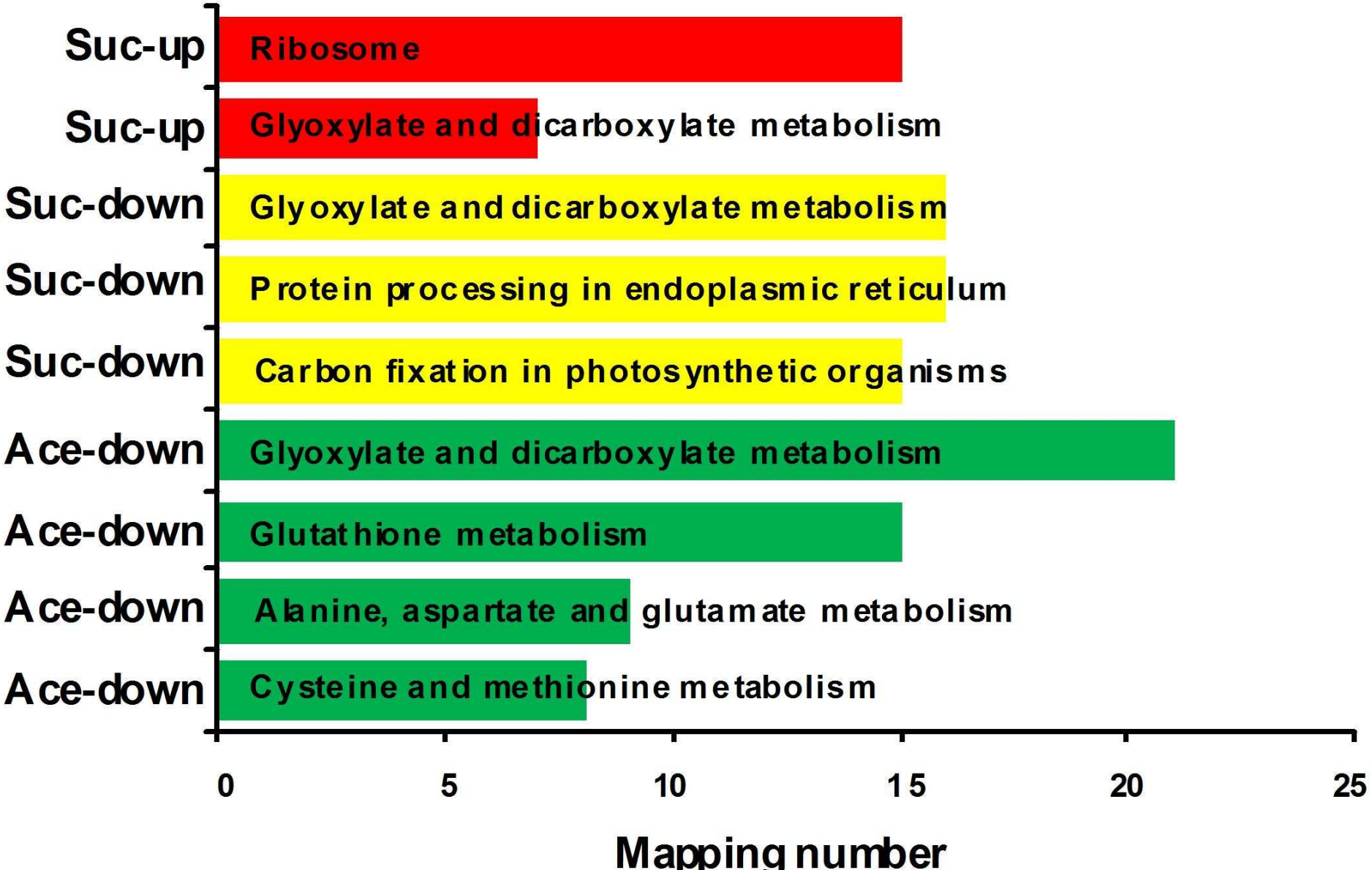
Suc-up
Ribosome
Suc-up
Glyoxylate and dicarboxylate metabolism
Suc-down
Glyoxylate and dicarboxylate metabolism
Suc-down
Protein processing in endoplasmic reticulum
Suc-down
Carbon fixation in photosynthetic organisms
Ace-down
Glyoxylate and dicarboxylate metabolism
Ace-down
Glutathione metabolism
Ace-down
Alanine, aspartate and glutamate metabolism
Ace-down
Cysteine and methionine metabolism
0
5
10
15
20
25
Mapping number

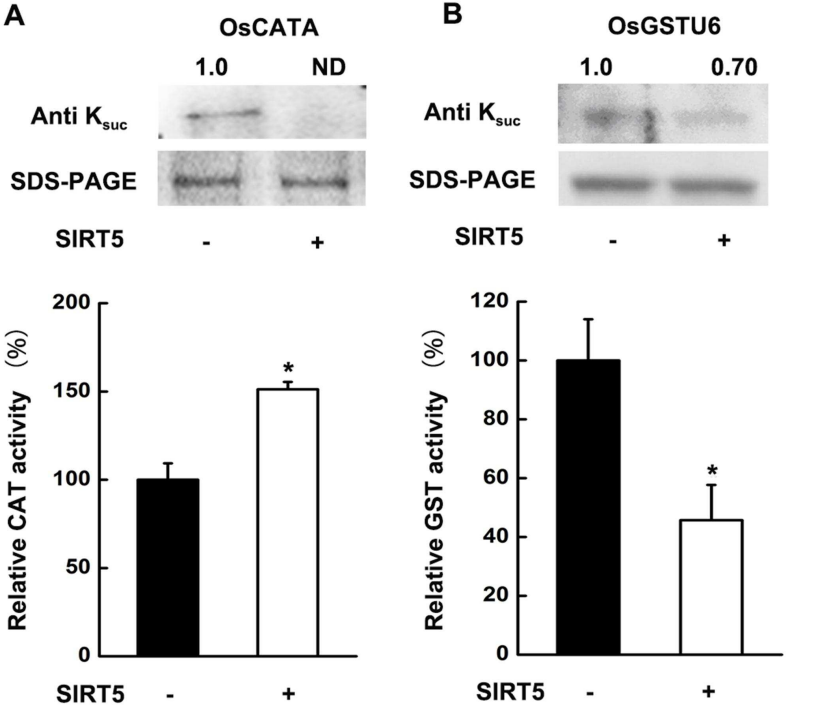
A
OsCATA
1.0
ND
Anti K_{suc}
SDS-PAGE
SIRT5
-
+
B
OsGSTU6
1.0
0.70
Anti K_{suc}
SDS-PAGE
SIRT5
-
+
Relative CAT activity (%)
200
150
100
50
0
*
SIRT5
-
+
Relative GST activity (%)
120
100
80
60
40
20
0
*
SIRT5
-
+